An Ultra-Wideband Common-Mode Suppression Filter Based on S-DBCSRR for High-Speed Differential Signals

Hao-Ran Zhu and Jun-Fa Mao, *Fellow, IEEE*

***Abstract*—In this letter, an ultra-wideband common mode filter is proposed for high-speed differential signal transmission. By etching a slot in the inner patch of a double slit complementary split ring resonator (S-DBCSRR), the noise rejection bandwidth can be expanded. The equivalent circuit model and surface current distribution are given to explain the working principle of the filter. From the simulated and measured results, it is found that the fractional bandwidth of the presented filter is 92% with a noise suppression level of 20 dB, and the differential signal can propagate with little degradation.**

***Index Terms*—Common-mode (CM) filter, complementary split ring resonator (CSRR), differential signal, wideband suppression.**

I. Introduction

In the modern mixed signal systems, the differential signal with its inherent immunity to noise, low crosstalk and low electromagnetic radiation has been widely applied. However, owing to the timing skew and amplitude unbalance along the differential signal path, the undesired common mode (CM) current would be induced, which can seriously deteriorate the signal integrity of the signal trace and cause electromagnetic interference problems. Therefore, wide and steep suppression of CM noise has attracted extensive attention in the design of high-speed differential signals [1].

Recently, many approaches have been reported to design wideband CM filters for differential signals. The CM chock with high permeability ferrite core is introduced in [2]. However, the operating frequency range is only validated around MHz as the permeability of the ferrite will reduce rapidly with the increase of frequency. In [3], a broadband and miniaturized CM noise suppression filter has been developed by using multilayer low-temperature co-fired ceramic technology. However, the cost is high owing to the complicated fabrication process. Some artificial structures such as planar electromagnetic bandgap structures are studied to design CM filters [4]–[7]. The complementary split ring resonator (CSRR) with an inherent filtering property has been widely applied in the microwave circuits and high-speed mixed signal systems [8], [9]. Recently, it was also demonstrated that the CSRRs are capable of mitigating the CM noise for microstrip differential line [10]. However, the operating bandwidth of the filter is narrow.

In this letter, a novel ultra-wideband (UWB) CM filter is proposed with double slit CSRR with slot (S-DBCSRR) for high-speed differential signal propagation. The CM noise can be suppressed from 1.52 GHz to 4.07 GHz under the rejection level of 20 dB, which is validated by measured and simulated results.

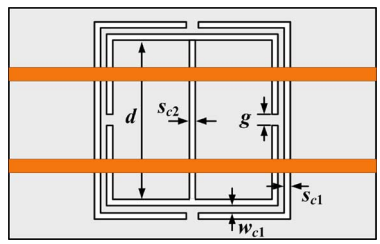

Fig. 1. The schematic of the proposed common mode filter with one S-DBCSRR.

II. Structure Design and Analysis

Fig. 1 shows the schematic of the differential line loaded with one S-DBCSRR unit cell. In order to keep the filter structure symmetric, the resonator is etched underneath the center of the transmission line. The corresponding geometric parameters of the S-DBCSRR are described, where d is the dimension of the inner square patch, g is the gap size of the split, s_{c1} and w_{c1} are the widths of the slot and the bridge, respectively. A slot is etched on the center of the inner patch with a width of s_{c2}.

As the structure is symmetric, the circuit model can be analyzed in the odd mode and the even mode excitation, respectively. In Fig. 2, L and C_g represent the equivalent inductor and grounded capacitor of the transmission line, respectively. L_m is the mutual inductance between the adjacent coupled lines. L_s and C_s are the equivalent inductance and capacitance of the S-DBCSRR in the ground plane. L_c and C_c are the equivalent inductance and capacitance which are introduced by etching a slot in the inner patch of the resonator.

From Fig. 2(a), the circuit is behaved as a transmission line with a grounded capacitor in the case of the odd mode. For the differential signals, the filter maintains the quasi-TEM mode

Manuscript received October 20, 2014; revised December 28, 2014; accepted February 01, 2015 Date of publication February 12, 2015; date of current version April 10, 2015. This work was supported by the National Natural Science Foundations of China under Grants 61234001 and 61361166010.

H.-R. Zhu is with the Key Lab of Ministry of Education for Research of Design and EMC of High Speed Electronic Systems, Shanghai Jiao Tong University, Shanghai, China, and also with the East China Research Institute of Electronic Engineering, Hefei, China (e-mail: hrzhu@sjtu.edu.cn).

J.-F Mao is with the Key Lab of Ministry of Education for Research of Design and EMC of High Speed Electronic Systems, Shanghai Jiao Tong University, Shanghai, China, and also with the State Key Laboratory of Complex Electromagnetic Environment Effects on Electronics and Information System, Shanghai, China (e-mail: jfmao@sjtu.edu.cn).

Color versions of one or more of the figures in this letter are available online at http://ieeexplore.ieee.org.

Digital Object Identifier 10.1109/LMWC.2015.2400914

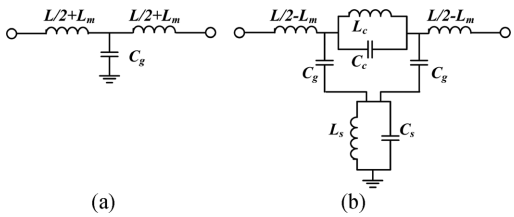

Fig. 2. The unit cell equivalent circuit for: (a) odd mode and (b) even mode.

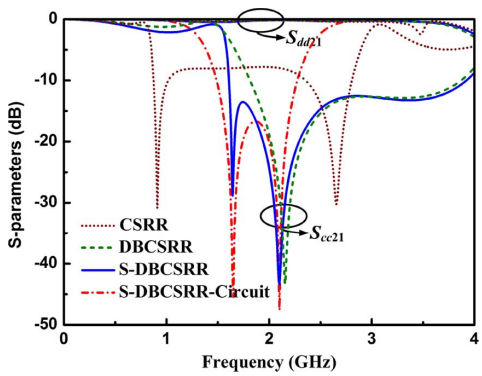

Fig. 3. Comparison of transmission behavior of the CM filter with different types of CSRR unit cell.

propagation within the operating frequency range. The electrical field distribution in the axial direction is weakened because the energy along the transmission line offset each other. Therefore, the differential signal can pass through with little interference. On the other hand, as shown in Fig. 2(b), a perfect magnetic wall is located in the center of the coupled line under the excitation of even mode. A transmission line loaded with an L_sC_s tank is achieved with S-DBCSRR, which is located in the ground plane. Moreover, by etching a slot in the inner patch of the resonator, an additional parallel L_cC_c resonator is also introduced between the transmission lines.

The transmission behavior of the common mode filter with different types of CSRR unit cell is shown in Fig. 3 for comparison. The geometrical sizes of resonator are listed: $d = 12$ mm, $w_{c1} = 0.4$ mm, $s_{c1} = 0.7$ mm, $s_{c2} = 0.7$ mm and $g = 0.4$ mm. The electrical properties of the used substrate are shown in Section III. In contrast with the traditional CSRR, the total inductance of the double slit CSRR is decreased with four parallel inductance of arms. Moreover, by etching a slot in the inner patch of the resonator, an additional transmission zero (TZ) is achieved in the stopband, which can broaden the noise rejection bandwidth. Under such circumstances, the CM noise coupling can be reduced efficiently with the S-DBCSRR while keeping the differential mode unaffected along the differential signal lines. The circuit simulation result of the filter with one S-DBCSRR is also depicted in the figure, from which we can see that the equivalent circuit predicts the transmission zeros correctly and gives pretty exact simulation results of S parameter at lower frequency. The values of lumped elements are followed as $L_e = 1.6$ nH, $C_e = 1.3$ pF, $L_s = 2.53$ nH, $C_s = 1.4$ pF, $L_c = 3$ nH and $C_c = 1.25$ pF. The locations of the two TZs can be adjusted with the variations of the circuit element values, which can preliminarily guide the filter design.

In Fig. 4, the surface current distributions of the CM current within the ground plane are plotted to interpret the noise suppression behavior. It is observed that the distribution of the solid

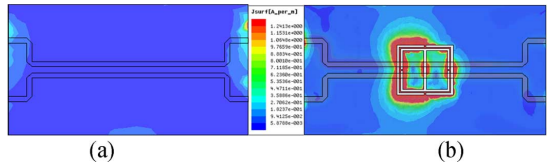

Fig. 4. Surface current distribution of (a) the reference board and (b) the proposed common mode filter at 2.1 GHz.

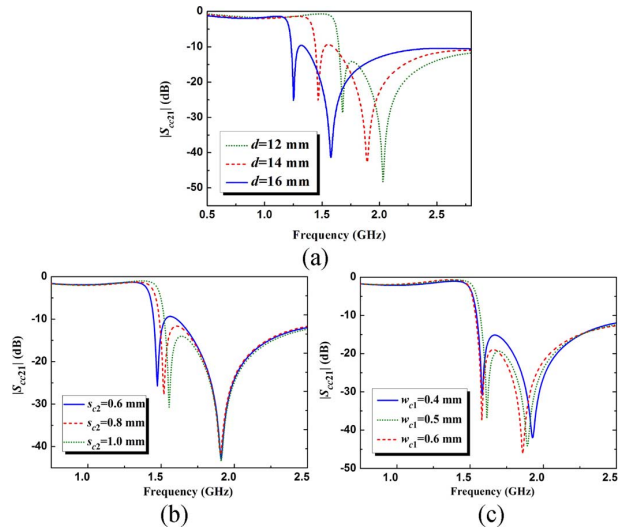

Fig. 5. The transmission behaviors of the CM filter with one S-DBCSRR for different parameter values of: (a) d, (b) s_{c2}, and (c) w_{c1}.

board has little disturbance. But, for the proposed filter, the surface current distribution at the resonate frequency of 2.1 GHz is obviously disturbed. The propagation of the CM noise can be prohibited sufficiently when the electromagnetic wave transmits across the S-DBCSRR within the board.

The simulated transmission behaviors of the CM filter with one S-DBCSRR for different values of d, s_{c2}, and w_{c1} are plotted in Fig. 5(a)–(c), respectively. As demonstrated in Fig. 5(a), it is obviously found that the lower cutoff frequency of the filter decreases with increasing of d. From Fig. 5(b), if the size of s_{c2} is decreased, the first TZ will move to the lower frequency, and then the second TZ keeps unchanged. Furthermore, as shown in Fig. 5(c), as w_{c1} increases, the second TZ moves to the lower frequency and the first one hardly changed.

According to the aforementioned discussions, the filter design procedure is summarized. First, for a given operating frequency range, the initial dimension of d is approximately equal to one-eighth wavelength of the lower cutoff frequency [8]–[10]. Then, in consideration of the mitigation level and the width of the stopband, the sizes of the slots such as, s_{c2} and w_{c1}, are employed to adjust the locations of the two TZs, respectively. For the filter with multi-order resonators, the adjacent resonators should be cascaded in order to enhance the electric coupling. Finally, the specific filter parameters can be optimized with the full wave EM simulator for the desired filter performance.

III. Results and Validation

To validate our design, a sample circuit is fabricated on Taconic RF-35 substrate with a relative permittivity of $\varepsilon_r = 3.5$, a loss tangent of $\tan\delta = 0.002$ and the substrate thickness of 0.762 mm. Based on the tradeoff between the circuit size and the filter performance, three resonators are employed to design the

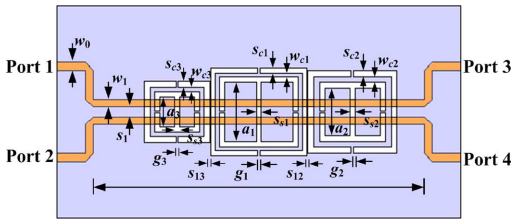

Fig. 6. Schematic of the proposed CM filter with three different S-DBCSRRs etched on the ground plane. Final structure parameters are: $a_1 = 14$ mm, $s_{c1} = 1$ mm, $w_{c1} = 0.8$ mm, $s_{s1} = 1$ mm, $g_1 = 0.5$ mm, $a_2 = 11.2$ mm, $s_{c2} = 1$ mm, $w_{c2} = 1.2$ mm, $s_{s2} = 1.1$ mm, $g_2 = 0.5$ mm, $a_3 = 7$ mm, $s_{c3} = 1$ mm, $w_{c3} = 0.9$ mm, $s_{s3} = 1.1$ mm, $g_3 = 0.5$ mm, $s_{12} = 0.2$ mm, $s_{13} = 0.2$ mm.

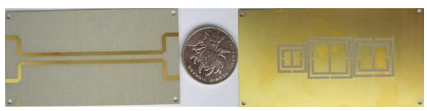

Fig. 7. Photograph of the fabricated prototype filter.

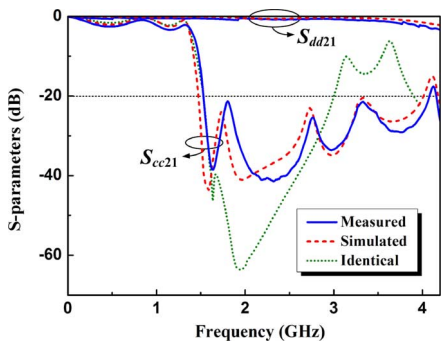

Fig. 8. Simulated and measured $|S_{21}|$ parameters of the differential mode and common mode signals.

TABLE I
COMPARISONS BETWEEN SOME PREVIOUS METHODS AND THE PROPOSED STRUCTURE FOR COMMON-MODE NOISE SUPPRESSION

Ref.	Used technology	*Size* ($\lambda_e \times \lambda_e$)	*FBW (%)* 10 dB	20 dB
[5]	HIS	0.26×0.16	60	24
[7]	UV DGS	0.44×0.44	87	---
[8]	Planar EBG	---	80	70
[11]	CSRR	0.43×0.14	54	37
	DSCSRR	0.64×0.13	51	41
This work	S-DBCSRR (same)	0.41×0.15	73	64
	S-DBCSRR (different)	0.43×0.15	109	92

λ_e represents the guided wavelength at the resonate frequency of even mode, FBW is the factional bandwidth.

filter with a reasonable noise reduction level. For the impedance matching, the differential line is designed with an odd-mode characteristic impedance of 50 Ω. The sizes of the differential line are calculated to be $w_0 = 1.7$ mm, $w_1 = 1.5$ mm, and $s_1 = 2$ mm. In modern high-speed differential circuit, an UWB CM noise suppression behavior is required. Three S-DBCSRRs with different resonate frequencies are etched on the ground plane. The schematic of the proposed CM filter is shown in Fig. 6.

The testing board is fabricated with standard PCB technology, and its prototype photograph is shown in Fig. 7. Four port vector network analyzer Agilent E5071C is utilized to measure the transmission responses of the proposed filter.

The measured transmission coefficients of the differential mode and common mode signals are both plotted in Fig. 8, with the simulated results given for comparison. The scattering parameter of the filter with identical resonators is also plotted in the figure. The noise rejection level is deepened as they resonate at the same frequency. For the case of different resonators, the bandwidth is broadened greatly as several *LC* resonators are cascaded together. From the figure, it is observed that the CM noise can be mitigated from 1.52 GHz to 4.07 GHz under the rejection level of 20 dB. The noise coupling can be reduced in UWB with a fractional bandwidth of 92%. In additional, the insertion loss of the differential signal is less than 0.8 dB from DC-3.5 GHz. The attenuation level is increased owing to the dispersion properties of the substrate at a higher frequency. Reasonable agreement is achieved between the simulated and measured results. Slight discrepancies are probably attributed to the tolerance in the fabricate process, the effect of the SMA connector and the lack of material uniformity.

Some comparisons between our design and previous works using different technologies are summarized in Table I. As shown in the table, both wide stopband and small structure size are achieved simultaneously with our design.

IV. CONCLUSION

In this letter, a novel UWB CM filter with S-DBCSRR is presented for high-speed differential signals. The mitigation characteristic of the resonator is improved by etching a slot in the inner patch of the double slit CSRR. Equivalent circuit model is developed to clarify the principle of the filter. The CM noise coupling can be reduced within a wide stopband when the differential signal is passed through with little degradation.

REFERENCES

[1] B. R. Archambeault, *PCB Design for Real-World EMI Control*. Norwell, MA: Kluwer, 2002.
[2] K. Yanagisawa, F. Zhang, T. Sato, K. Yanagisawa, and Y. Miura, "A new wideband common-mode noise filter consisting of Mn-Zn ferrite core and copper/polyimide tape wound coil," *IEEE Trans. Magn.*, vol. 41, no. 10, pp. 3571–3573, Oct. 2005.
[3] B.-C. Tseng and L.-K. Wu, "Design of miniaturized common-mode filter by multilayer low-temperature co-fired ceramic," *IEEE Trans. Electromagn. Compat.*, vol. 46, no. 4, pp. 571–579, Nov. 2004.
[4] F. de Paulis, L. Raimondo, S. Connor, B. Archambeault, and A. Orlandi, "Compact configuration for common-mode filter design based on planar electromagnetic bandgap structures," *IEEE Trans. Electromagn. Compat.*, vol. 54, no. 3, pp. 646–654, Jun. 2012.
[5] C.-H. Tsai and T.-L. Wu, "A broadband and miniaturized common-mode suppression filter for gigahertz differential signals based on negative permittivity metamaterials," *IEEE Trans. Microw. Theory Tech.*, vol. 58, no. 1, pp. 195–202, Jan. 2010.
[6] S.-J. Wu, C.-H. Tsai, T.-L. Wu, and T. Itoh, "A novel wideband common-mode suppression filter for gigahertz differential signals using coupled patterned ground structure," *IEEE Trans. Microw. Theory Tech.*, vol. 57, no. 4, pp. 848–855, Apr. 2009.
[7] J. H. Choi, P. W. C. Hon, and T. Itoh, "Dispersion analysis and design of planar electromagnetic bandgap ground plane for broadband common mode suppression," *IEEE Microw. Wireless Compon. Lett.*, vol. 24, no. 11, pp. 772–774, Nov. 2014.
[8] R. Marques, F. Martin, and M. Sorolla, *Metamaterials With Negative Parameters: Theory, Design, and Microwave Applications*. New York: Wiley, 2007.
[9] H. R. Zhu, J. J. Li, and J. F. Mao, "Ultra-wideband suppression of SSN using localized topology with CSRRs and embedded capacitance in high-speed circuits," *IEEE Trans. Microw. Theory Tech.*, vol. 61, no. 2, pp. 764–772, 2013.
[10] J. Naqui, A. Fernandez-Prieto, M. Duran-Sindreu, F. Mesa, J. Martel, F. Medina, and F. Martin, "Common-mode suppression in microstrip differential lines by means of complementary split ring resonators: Theory and applications," *IEEE Trans. Microw. Theory Tech.*, vol. 60, no. 10, pp. 3023–3034, Oct. 2012.